Rapid Solid-State Synthesis of Titanium Aluminides

Richard G. Blair,[†] Edward G. Gillan,[‡] Ngoc Kim B. Nguyen,[†]
Dominick Daurio,[†] and Richard B. Kaner*,[†]

*Department of Chemistry and Biochemistry and Exotic Materials Institute,
University of California − Los Angeles, Los Angeles, California 90095-1569,
and Department of Chemistry and the Optical Science and Technology Center,
University of Iowa, Iowa City, Iowa 52242-1294*

Received January 9, 2003. Revised Manuscript Received April 29, 2003

Intermetallics, such as the titanium aluminides, hold promise for high-temperature structural applications if their ductility can be improved by making fine-grained materials. An important step toward this goal is the rapid synthesis of finely divided powders via simple chemical processes. Here, single-displacement reactions between varying ratios of the metal halides $TiCl_3$ and $AlCl_3$, utilizing Mg as a reducing agent, enables the rapid synthesis of Ti_3Al, TiAl, and $TiAl_3$ upon initiation with a heated filament. Reaction temperatures and propagation rates are measured using in situ thermocouples and electrodes. This leads to insights into the propagation mechanism for intermetallic formation in these displacement reactions. Once the sublimation temperature of $AlCl_3$ (178 °C) is reached, propagation accelerates rapidly. The reaction temperature exceeds 1000 °C within 700 ms. Propagation velocities on the order of 0.5 mm/s are observed. Redox reactions that begin during propagation create electrical signals, which confirm that initiation of chemical processes occur upon the sublimation of $AlCl_3$. Microwave heating was found to be another effective method to initiate these reactions and leads to the formation of phase pure TiAl which is not obtainable as a single product via filament initiation. Powders of $TiAl_3$ can also be produced through reactions between LiAl and $TiCl_3$.

Introduction

High-temperature intermetallic compounds have shown promise over the last several decades as materials for use in modern aircraft, as high-temperature engine components, in shape-memory devices, and as lightweight structural supports.[1,2] One important drawback to their use is that most of these compounds are brittle at low temperatures.[3,4] It has been suggested that the brittleness arises from the nature of the metallic bonding in these intermetallics.[5,6] There have been various reports over the past decade for evidence of improved ductility in fine grained [7−9] or nanocrystalline[10−12] materials.

The traditional synthesis of these intermetallic compounds involves arc or induction melting of the elements, followed by high-temperature annealing which leads to a coarse-grained product. Alternative techniques such as rapid solidification of a metallic melt[13] and high-energy ball milling[14,15] can produce fine powders in crystalline or amorphous form, respectively. Another method known as self-propagating high-temperature synthesis (SHS) has shown some promise in the synthesis of alloys.[16−20] There are reports of reactions between fine powders of titanium and aluminum to form intermetallic compounds in the Al−Ti[21] system. In contrast to many other SHS reactions, this alloy system generally is not very energetic, and the entire sample must be preheated to at least 700 °C before a self-propagating reaction occurs. The theoretical maximum reaction temperatures for metal alloy synthesis are also generally lower (700−1700 °C) than most of those for ceramic-forming SHS reactions (1900−4500 °C).[16,22]

---

[*] To whom correspondence should be addressed. kaner@chem.ucla.edu.

[†] University of California − Los Angeles.

[‡] University of Iowa.

(1) Dimiduk, D. M. *Mater. Sci. Eng., A* **1999**, *A263*, 281−288.
(2) Dimiduk, D. M.; Miracle, D. B. *Mater. Res. Soc. Symp. Proc.* **1989**, 349−359.
(3) Fleischer, R. L. *J. Mater. Sci.* **1987**, *22*, 2281−2288.
(4) Pope, D. P. *Mater. Res. Symp. Proc.* **1987**, *81*, 3−11.
(5) Sauthoff, G. *Z. Metall.* **1989**, *80*, 337.
(6) Fleischer, R. L.; Dimiduk, D. M.; Lipsitt, H. A. *Annu. Rev. Mater. Sci.* **1989**, *19*, 231−263.
(7) Schulson, E. M.; Barker, D. R. *Scr. Metall.* **1983**, *17*, 519−522.
(8) Hahn, K. H.; Vedula, K. *Scr. Metall.* **1989**, *23*, 7−12.
(9) Matsugi, K.; Wenman, D. W.; Stoloff, N. S. *Scr. Metall. Mater.* **1992**, *27*, 1633−1638.
(10) Haubold, T.; Bohn, R.; Birringer, R.; Gleiter, H. *Mater. Sci. Eng., A* **1992**, *A153*, 679−683.
(11) Chang, H.; Höffler, J.; Altstetter, C.; Averback, R. *Mater. Sci. Eng. A* **1992**, *A153*, 676−678.
(12) Wang, Y.; Chen, M.; Zhou, F.; Ma, E. *Nature* **2002**, *419*, 912−915.
(13) Reichman, S.; Chang, D. S. *Superalloys II: High Temperature Materials for Aerospace and Industrial Power*; John Wiley and Sons: New York, 1987.
(14) Koch, C. C. *Annu. Rev. Mater. Sci.* **1989**, *19*, 121−143.
(15) Tomasi, R.; Pallone, E. M. J. A.; Botta F, W. J. *Mater. Sci. Forum* **1999**, *312−314*, 333−338.
(16) Hardt, A. P.; Holsinger, R. W. *Combust. Flame* **1973**, *21*, 91−97.
(17) Munir, Z. A.; Anselmi-Tamburini, U. *Mater. Sci. Rep.* **1989**, *3*, 277−365.
(18) Munir, Z. A.; Odink, D. A. In *Metallurgical Processes for the Early Twenty-First Century*; Sohn, H. Y., Ed.; The Minerals, Metals, and Materials Society: Warrendale, PA, 1994; pp 167−187.
(19) Kopit, Y. *Intermetallics* **2001**, *9*, 387−393.
(20) Hirota, K.; Nakane, S.; Yoshinaka, M.; Yamaguchi, O. *Int. J. Self-Propag. High-Temp. Synth.* **2002**, *10*, 345−358.
(21) Wright, R. N.; Rabin, B. H.; McFerran, W. H. *J. Mater. Res.* **1992**, *7*, 2733−2738.

10.1021/cm021829a CCC: $25.00

Unconventional synthetic routes to intermetallic compounds have been suggested as a way to explore morphological and grain-size effects on the physical properties of these systems that are difficult to access by conventional methods.[6] These include solution-phase methods[23−25] and the reduction of solid precursors.[26] These could also include single- and double-displacement reactions. For example, the classic single-displacement reaction between aluminum and a metal oxide, known as the thermite reaction, is highly exothermic because a stable byproduct, Al_2O_3, is produced. Single-displacement reactions such as the co-reduction of metal oxides have been accomplished using Li, Mg, or Ca as reducing agents to produce nickel intermetallic phases.[27] Such reactions often result in a product contaminated by alkali or alkaline earth metal oxides. These can be difficult to remove while still maintaining the integrity of the intermetallic powder formed.

A more recent method involving double-displacement reactions, termed solid-state metathesis (SSM), has shown promise in the rapid synthesis of a wide range of crystalline refractory ceramics[28−30] and other inorganic solids.[31−34] Solid-state metathesis reactions have demonstrated control over crystallite size,[35] as well as the ability to form solid-solutions and ceramic composites.[36]

The use of metal halides as starting materials instead of metal oxides allows greater control over the reaction. Individual reactions can be tuned to attain higher or lower temperatures depending on which metals are employed as reducing agents and which halides are used. These reactions generally have an upper temperature limit of the boiling point of the salt produced. The lower limit is dictated by the reaction dynamics and heat-transfer characteristics of the reaction vessel.

The availability of metal halides offers a potentially inexpensive route to intermetallic powders. For example, titanium is typically prepared by converting the ore to the tetrachloride and then purifying this halide and reducing it to the metal with magnesium. This is known as the Kroll process.[37] Co-reduction of titanium halides with other metal halides could be used to produce fine powders of intermetallic phases directly. This would eliminate a step in the processing of titanium ore and potentially reduce the cost of subsequently producing intermetallic alloys.

In this report, we examine another type of single-displacement reaction that uses metal halides, and, analogous to SSM reactions, is driven by the formation of stable salts. With a suitable metal as a reducing agent, for example magnesium, the resulting products consist of co-reduced metals in a solidified $MgCl_2$ matrix. After washing away the salt, fine powders are obtained. The effects of microwave heating and comparison to double-displacement reactions is also described.

Experimental Section

Metal Aluminide Reagents. The following reagents were used as received: $TiCl_3$ (aluminum reduced 98+%, 77.6% α-$TiCl_3$, remainder $AlCl_3$; Strem), $AlCl_3$ (99.99+%; Strem), Mg powder (99%; Strem), $MgCl_2$ (ultra dry, 99.9%, Alpha Aesar), $TiCl_3$ (99%, Aldrich), and TiI_4 (99.9%, Gelest).

LiAl was synthesized by melting lithium (99.9%+, Aldrich) and aluminum (ESPI 99.99%, 325 mesh) in a steel crucible at 800 °C for 2 h under a helium atmosphere. The melt was rapidly cooled, ground in an agate mortar and pestle, and characterized by XRD.

Safety. *Caution! These reactions reach significant temperatures. Care should be taken in the choice of a reaction vessel and when increasing the scale of the reaction. Safety precautions for specific steps of the experiment are also noted in the appropriate sections.*

Metal Aluminide Synthesis. Experiments to produce Ti_3Al_x were conducted in a helium filled drybox. The metal halides and magnesium for these reactions were ground in a planetary ball mill (Fritsch Pulverizette 7) at 600 rpm for 10 min. Enough reagents were milled at a time for four (approximately 1 g) reactions. This was to ensure powder uniformity for multiple reactions of the same type. A rapid exothermic reaction between these intimately mixed precursors was initiated by brief exposure to a heated filament. The specific reactor geometry is described in detail below.

The products were transferred to a Schlenk flask while in the drybox. The products were initially stirred with 50 mL of dry ethanol under nitrogen. After the initial rinse, the products were allowed to come in contact with air. Isolation of the products was completed by rinsing twice more with ethanol, each rinse followed by centrifugation and drying under vacuum. The resulting powder was then characterized by XRD.

To avoid oxygen contamination, samples were isolated by transferring the product to a Soxhlet extractor while in the drybox. The apparatus was removed from the drybox and the sample was extracted with dry *N*,*N*-dimethyl formamide (DMF) while under nitrogen. Dry DMF was prepared by refluxing ~100 mL of solvent over 5 g of CaH_2. This mixture was transferred to the Soxhlet extraction apparatus. The calcium hydride was left in the solvent to ensure that no water was present during the isolation process. The solvent was heated to boiling and the extraction was performed under a slight overpressure of nitrogen. After 12 h of extraction, the product was held under dynamic vacuum for 4 h to dry the sample and then transferred back to the helium filled drybox. The isolated product was removed from the extraction thimble and stored under helium.

Microwave Synthesis. Reactions initiated by microwave energy were carried out in a 500-W Panasonic household microwave oven (2.45 GHz) with an alumina disk as a reaction platform. In a He-filled glovebox, reaction mixtures were

---

(22) Yi, H. C.; Moore, J. J. *J. Mater. Sci.* **1990**, *25*, 1159−1168.

(23) Haber, J. A.; Gunda, N. V.; Balbach, J. J.; Conradi, M. S.; Buhro, W. E. *Chem. Mater.* **2000**, *12*, 973−982.

(24) Haber, J. A.; Gunda, N. V.; Buhro, W. E. *J. Aerosol Sci.* **1998**, *29*, 637−645.

(25) Bonnemann, H.; Brijoux, W.; Hofstadt, H.-W.; Ould-Ely, T.; Schmidt, W.; Wassmuth, B.; Weidenthaler, C. *Angew. Chem., Int. Ed.* **2002**, *41*, 599−603.

(26) Vie, D.; Valero, N.; Martinez, E.; Sapina, F.; Folgado, J.-V.; Beltran, A. *J. Mater. Chem.* **2002**, *12*, 1017−1021.

(27) Itagaki, K.; Endo, S.; Kobayashi, H.; Satake, H. In *Metallurgical Processes for the Early Twenty-First Century*; Sohn, H. Y., Ed.; The Minerals, Metals, and Materials Society: Warrendale, PA, 1994; pp 205−217.

(28) Gillan, E. G.; Kaner, R. B. *J. Mater. Chem.* **2001**, *11*, 1951−1956.

(29) Parkin, I. P.; Nartowski, A. T. *J. Mater. Sci. Lett.* **1999**, *18*, 267−268.

(30) Gillan, E. G.; Kaner, R. B. *Chem. Mater.* **1996**, *8*, 333−343.

(31) Cumberland, R. W.; Blair, R. G.; Wallace, C. H.; Reynolds, T. K.; Kaner, R. B. *J. Phys. Chem. B* **2001**, *105*, 11922−11927.

(32) O'Loughlin, J. L.; Wallace, C. H.; Knox, M. S.; Kaner, R. B. *Inorg. Chem.* **2001**, *40*, 2240−2245.

(33) Jarvis, R. F., Jr.; Jacubinas, R. M.; Kaner, R. B. *Inorg. Chem.* **2000**, *39*, 3243−3246.

(34) Bonneau, P. R.; Wiley, J. B.; Kaner, R. B. *Inorg. Synth.* **1995**, *30*, 33−37.

(35) Bonneau, P. R.; Jarvis, R. F., Jr.; Kaner, R. B. *Nature (London)* **1991**, *349*, 510−512.

(36) Rao, L.; Gillan, E. G.; Kaner, R. B. *J. Mater. Res.* **1995**, *10*, 353−361.

(37) Greenwood, N. N.; Earnshaw, A. In *Chemistry of the Elements*; Pergamon Press: New York, 1984; p 1112.

placed in tightly capped 20-mL borosilicate vials. The mixtures were then removed from the glovebox and microwave energy was applied at the 100% power setting. The reaction initiated after approximately 3 min of applied energy. Input of energy was ceased upon observation of reaction initiation. *Caution: continued input of microwave energy can lead to severe discharges in the microwave cavity.* The products were isolated using the same workup outlined in the previous section.

Metathesis Reactions. Experiments to produce $TiAl_3$ via metathesis were conducted in a helium filled drybox. $TiCl_3$ and LiAl were measured out in a ratio of 1:3. Typically enough reagents were used to yield a reaction mass of 1 g. These reactants were ground in an agate mortar. *Caution: this reaction mixture may be initiated by frictional heating from the grinding process.* The ground reagents were placed in a steel reaction vessel modeled after a bomb calorimeter.[36] The reaction was initiated with a resistively heated Nichrome wire. The products were washed with ethanol and isolated with vacuum filtration.

Characterization. The products were analyzed using a Crystal Logic $\theta-2\theta$ powder X-ray diffractometer with Cu Kα radiation ($\lambda = 1.5418$ Å). Product samples were scanned from 10 to 100° 2θ at 0.1-degree intervals with a 3-s count time per interval. The patterns obtained were then analyzed and interpreted using the Macintosh software MacDiff (http://www.geol.uni-erlangen.de/html/software/Macdiff.html).

Semiquantitative analysis was conducted using energy-dispersive X-ray analysis (EDX) performed on a Cambridge Stereoscan 250 scanning electron microscope. Analysis was performed using a Kevex Sigma system equipped with a Kevex super beryllium window (5 μm thick).

Oxygen content was assessed by using energy-dispersive X-ray analysis (EDX) performed on a JEOL JSM 840 scanning electron microscope. Analysis was performed using a Phoenix system operating in windowless mode.

The titanium compositions of the alloys were determined by X-ray fluorescence spectrometry (XRF). Analysis was carried out using a Philips Norelco X-ray fluorimeter with Mo Kα ($\lambda = 0.710749$ Å) as the excitation source. The fluorescence X-rays were diffracted with a Pentaerythritol tetrakis(hydroxymethyl)-methane (PET) analyzer crystal. The mass percent of titanium in each product was measured by monitoring Ti Kα ($\lambda = 2.75$ Å) radiation and comparing it to a standard curve generated from known masses of titanium. Titanium powder, used for the external standards curve, was synthesized via a single-displacement reaction: $TiI_{4(s)} + 2\ Mg_{(s)} \rightarrow Ti_{(s)} + 2\ MgI_{2(s)}$. The product of this reaction was washed with dry ethanol to remove the salt byproduct and dried under vacuum. It was necessary to synthesize titanium by this method to produce a standard with particle size similar to the titanium−aluminum alloys produced. The sample was examined for Mg content with a rubidium biphthalate (RAP) analyzer crystal. No Mg or I were detected in this product by XRF.

Thermogravimetric analyses (TA instruments model 2950) were performed on washed products. The samples were loaded onto a platinum pan and heated in either an air or argon atmosphere.

Thermal Propagation Profiling. The Ti_3Al precursor mixture was loaded into a specially constructed vessel designed to allow measurement of the reaction temperature as it propagated.[31] Four sets of thermocouples were alternated with four sets of platinum electrodes at 0.5-cm intervals (Figure 1). The electrodes were used to monitor any electric fields produced by the reaction.

These profiling reactions were initiated by applying current to a Nichrome wire embedded in the reaction mixture. Initiation was controlled and monitored by a computer running a custom control program.[31] Data were taken at either 0.5- or 1-ms intervals.

Results

Titanium Aluminide Synthesis. The formation of intermetallic compounds in the Ti−Al system was investigated by varying the molar ratio of aluminum to titanium. This was accomplished by adding increasing amounts of aluminum chloride to Al reduced $TiCl_3$ ($3TiCl_3 \cdot AlCl_3$). The general equation for these reactions is

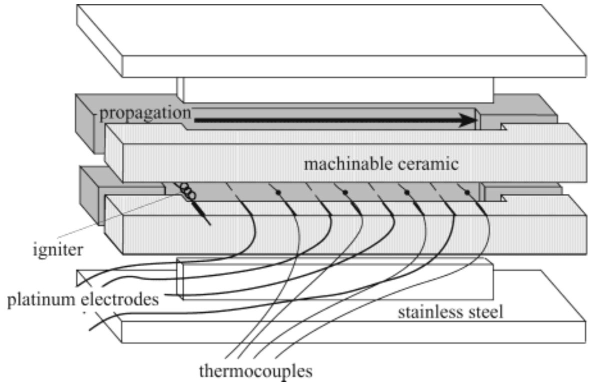

Figure 1. Reaction cell for determining reaction propagation rates, electrical field production, and the maximum reaction temperature (T_{max}). The outer two pieces are constructed of 308 stainless steel. The inner pieces are constructed of machineable aluminum silicate.

$$3\,TiCl_3 + nAlCl_3 + (3n + 9)/2\,Mg \rightarrow 3\,Ti\cdot nAl + (3n + 9)/2\,MgCl_2 \quad (1)$$

Note that in Equation 1 the product is expressed as 3 mol of titanium and n mol of aluminum; however, in most cases, the product actually consists of more than one titanium−aluminum, Ti_xAl_y, intermetallic phase. Reactions with 0−23 mol of aluminum chloride were explored. The finely ground powder mixtures were initiated by brief heating with a Nichrome wire. The results are summarized in Table 1. This range accessed portions of the Ti−Al phase diagram containing Ti_3Al, TiAl, $TiAl_2$, and $TiAl_3$.[38]

For reactions containing both titanium and aluminum, the products included five major phases: Ti, Ti_3Al, TiAl, $TiAl_3$, and Al, as identified by powder X-ray diffraction. By $n \geq 8$, more aluminum-rich phases are dominant until only $TiAl_3$ and Al were detected in the product. As crystallinity of the product can vary, XRD does not give a true quantitative measure of the bulk composition of the powder produced. To determine the composition of each product, X-ray fluorescence spectrometry was used to measure the titanium content in the samples, as reported in Table 1.

Adsorption of atmospheric water on the surfaces of the product would result in a measured mass percent of titanium that is lower than expected. The powders produced were found to pick up large quantities of water upon exposure to air. The error induced by water content was reduced by heating the alloys to 60 °C in vacuo for several days. As a further test, the samples were heated in vacuo at 300 °C for 2 h. The XRF results were unchanged, indicating that heating at 60 °C was sufficient.

Microwave Synthesis. Microwave-induced solid-state single-displacement reactions were studied by utilizing 3Ti·Al reaction mixtures. The resulting prod-

---

[38] Massalski, T. B. *Binary Alloy Phase Diagrams*; 2nd ed.; ASM Intl: Parks, OH, 1990.

Table 1. Phase Composition of Ti−Al Forming Single-Displacement Reactions

reactant metal molar ratio (Ti/Al)	measured % Ti in sample[b]	expected % Ti in sample	crystalline products[a]	
			from Nichrome wire initiation	from microwave initiation
3:0	100 ± 4	100	Ti	Ti
3:1	63 ± 3	84	Ti, Ti_3Al	**Ti**, Ti_3Al
3:1.4	73 ± 2	80	**Ti**, **Ti_3Al**, TiAl *(tr)*	
3:2	64 ± 3	72	**Ti_3Al**, **TiAl** Ti *(tr)*	**Ti_3Al**, TiAl *(tr)*, Ti_9Al_{23} (tr)
3:3	66 ± 3	64	Ti_3Al, **TiAl**	Ti_3Al, **TiAl**, $TiAl_3$ *(tr)*, Ti_9Al_{23} *(tr)*
3:4	43 ± 2	57	Ti_3Al, **TiAl**,$TiAl_3$, Ti_9Al_{23} *(tr)*	Ti_3Al
3:5	48 ± 5	52	Ti_3Al, **TiAl**, **$TiAl_3$**	**Ti_3Al**, **TiAl**, $TiAl_3$ *(tr)* Ti_9Al_{23} *(tr)*
3:6	43 ± 2	47	TiAl,**$TiAl_3$**,Ti_3Al *(tr)*	**TiAl,Ti_3Al**,TiAl *(tr)*
3:7	43 ± 2	43	TiAl, **$TiAl_3$**, Ti_3Al *(tr)*	TiAl
3:8	43 ± 2	40	**$TiAl_3$**, Al, TiAl *(tr)*,Ti_3Al*(tr)*	**TiAl**,Al, Ti_3Al *(tr)*,$TiAl_3$ *(tr)*
3:9	30 ± 2	37	**$TiAl_3$**, TiAl *(tr)*, Ti_3Al*(tr)*	TiAl
3:10	34 ± 2	35	**$TiAl_3$**, Al	**TiAl**, $TiAl_3$ *(tr)*
3:20	24 ± 1	21	**$TiAl_3$**, Al	

[a] Major phases present are in bold. *(tr)* = trace. [b] Titanium content was determined by X-ray fluorescence.

ucts were compared to the same reaction mixture initiated with a Nichrome wire. Different phase compositions than that produced by Nichrome wire initiation were obtained. Table 1 illustrates the differences in phase composition between the same reactions utilizing different initiation methods.

The product produced by this type of reaction, whether the initiation is by microwave or filament, is a very fine powder. By themselves, both finely divided titanium and aluminum are readily oxidized. Therefore, care was taken to minimize water and oxygen contact with the products. Even with such precautions, some compositions may be more easily oxidized than others. However, no oxygen was detected in freshly isolated samples of 3Ti·Al and 3Ti·5Al by EDX. Oxygen content can be controlled by using dry, oxygen free *N*,*N*-dimethyl formamide (DMF) as a solvent for the $MgCl_2$ byproduct. By using the method described in the Experimental Section, powders completely free from oxygen can be prepared.

Single-displacement reactions were also performed separately with only $TiCl_3$ and with only $AlCl_3$. The reaction between $AlCl_3$ and 1.5 Mg did not propagate in the reaction cell. The reaction could be forced to propagate by using microwave initiation. The reaction with purchased α-$TiCl_3$ was self-propagating and produced pure Ti as determined by XRD.

Reactions involving $TiCl_3$ produce both macroscopic- and microscopic-scale filaments, as can be seen in Figure 2. These filaments represent approximately 10% of the bulk product produced, with the remainder being particles of the same micrometer-sized scale as the filaments. This result is typical of all Ti−Al forming reactions.

Metathesis Route. LiAl can also be used as a precursor to Ti−Al intermetallics in solid-state metathesis (SSM) reactions. Reacting LiAl with $TiCl_3$ results in rapid self-propagating reactions yielding fine, gray powders after washing. The general balanced chemical reaction is

$$TiCl_3 + 3LiAl \rightarrow Ti \cdot 3Al + 3LiCl \qquad (2)$$

Analysis of the product by XRD indicates that the crystalline phase generated from eq 2 is $TiAl_3$. Direct measurements of the reaction temperature profile in the $TiCl_3$/LiAl system were recorded with an in situ thermocouple. The peak temperature is 1300 °C and occurs within 0.26 s after ignition; this is comparable to the temperature rise observed in single-displacement reactions. The cooling curve is also quite fast, with temperatures dropping below the melting point of the LiCl byproduct (mp = 610 °C) within 8 s.

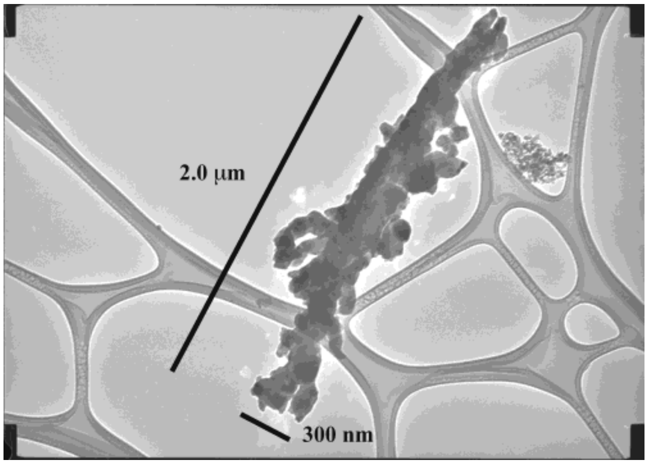

Figure 2. A Ti/Al microfilament, formed from a single-displacement reaction with a molar ratio of $TiCl_3$/$AlCl_3$/Mg 3:1:6, as viewed by transmission electron microscopy.

Scanning electron microscopy was performed on samples of the $TiAl_3$ product before and after washing. After washing, the product resembles a mass of spheroidal particles in the submicrometer to 10 micrometer range. The spherical particle morphology suggests that these compounds are melted at some point in their formation or that they have formed from a molten metallic state. EDX analysis of the washed product gives a Ti/Al ratio of 1:3.33 which is consistent with the results from the single-displacement reaction product.

Thermogravimetric analysis on the $TiAl_3$ product shows that when heated in either argon or air to 1000 °C, there is a weight gain beginning around 700 °C, although the XRD of the product afterward showed no evidence of Al_2O_3 or TiO_2. This is comparable to conventionally synthesized material which shows oxidation beginning around 800 °C.

Thermal Propagation Profiles. To better understand the mechanism of propagation of the single-displacement reactions, all reactions were performed in a specially designed reaction vessel that allowed real-time monitoring of the reaction by temperature profiles and electrical measurements (see Figure 1). Figure 3 shows the thermal profiles from four thermocouples embedded in a reaction mixture with the reactant ratio

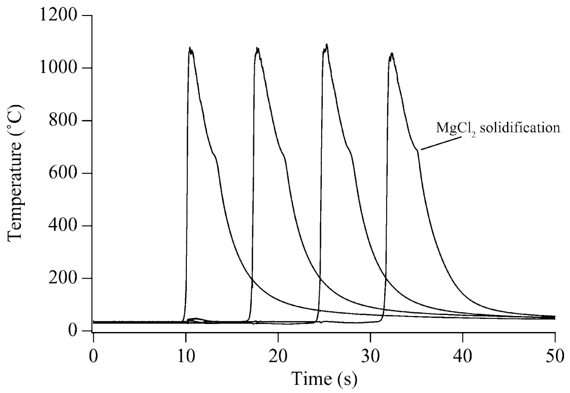

Figure 3. Representative set of thermal profiles for a solid-state single-displacement reaction. Here, four K-type thermocouples were embedded in a $TiCl_3/AlCl_3/Mg$ 3:1:6 reaction mixture and spaced at 1-cm intervals. The kink in the cooling portion of each curve is due to the solidification of $MgCl_2$.

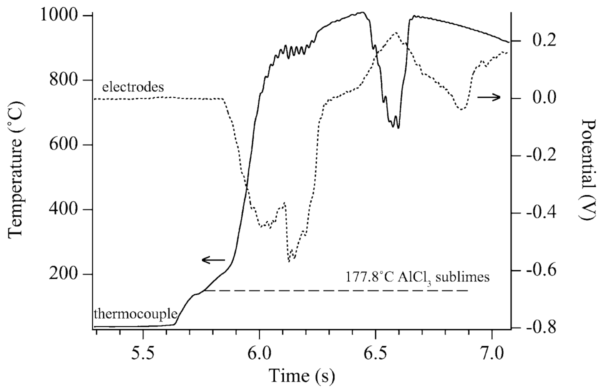

Figure 4. Thermal and electrical profiles of the single-displacement reaction between $TiCl_3/AlCl_3/Mg$ 3:23:39. The reaction heats rapidly once $AlCl_3$ changes phase at 177.8 °C. The electrical signal from the platinum electrode indicates when chemical processes commence.

of $TiCl_3/AlCl_3/Mg$ 3:1:6. The reaction was initiated after 1 s to establish a baseline temperature. Power was applied to the Nichrome wire for 4 s. The themocouples were spaced at 1-cm intervals starting 1.5 cm from the Nichrome wire. Visual inspection of the reaction showed that the reaction zone was very narrow (typically under 1 mm long). If the maximum temperature of each profile is used as an indicator of the position of the reaction front, it can be seen that a typical reaction takes about 40 s to propagate through the cell. For this example, the propagation rate is on the order of 1.4 mm/s. Increased aluminum content in the reaction mixture resulted in slower propagation rates and less uniform propagation.

Along with thermocouples, platinum electrodes were embedded in the reaction mixture. These electrodes were also used as a further gauge of propagation rate. A potential can be measured between two opposite electrodes as the reaction front intersects them. The continued use of the same platinum electrodes in subsequent reactions resulted in a degraded signal. It was found that physically abrading the surface of the electrode or removing the portions that were in the reaction mixture improved the signal of the electrodes in new reactions.

Electrodes and thermocouples that were embedded in reacted portions of the mixture were found to respond to fields produced by the reaction front intersecting thermocouples or electrodes further along the propagation path. Figure 4 illustrates this phenomenon. The signal from a platinum electrode is overlaid with the signal from a thermocouple positioned 0.5 cm further along the reaction path. The reaction front is intersecting the thermocouple, but a response can be seen from the electrode as well.

Additionally, the width of these pulses is significantly smaller than the temperature profile. Figure 5 shows a typical electrode response. The reaction front has intersected with electrode 2 and a signal is also evident from electrode 1 (in the reacted portion of the mixture). Electrodes 3 and 4, which are embedded in unreacted portions of the mixture at this point, do not exhibit any signal. The reaction in Figure 3 with a reactant ratio of $TiCl_3/AlCl_3/Mg$ 3:1:6 was found to possess a propagation rate of 1.43 mm/s. This corresponds to a reaction zone with a width of 0.53 mm and a reaction volume of 0.081 mm^3 as calculated from the width of the electrode signals.

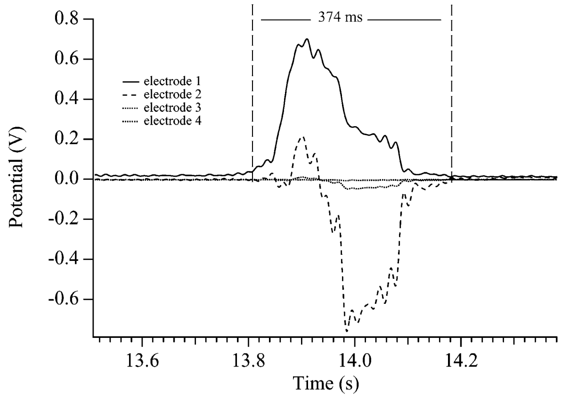

Figure 5. Electrical profile of a $TiCl_3/AlCl_3/Mg$ 3:1:6 displacement reaction, showing the 374-ms duration of the process. The reaction snapshot shown has propagated past electrodes 1 and 2, hence the electrodes' response; but it has not yet reached electrodes 3 and 4.

Discussion

Titanium−Aluminum Synthesis. The formation of titanium aluminum intermetallic compounds via single-displacement reactions was explored for two main reasons. First, these compounds are industrially important for structural applications (Ti_3Al and $TiAl_3$), and potentially for hydrogen storage (TiAl).[13] Second, an inexpensive source of the metal halide precursor, $3TiCl_3 \cdot AlCl_3$ (a mixture of $TiCl_3$ and $AlCl_3$ produced by reducing liquid $TiCl_4$ with aluminum metal), is available because it is often used in Zeigler-Natta catalysis. Hence, a thorough study of the titanium−aluminum system through single-displacement reactions can be carried out at relatively low cost. The factors affecting the formation of various titanium−aluminum intermetallic compounds were investigated by performing a series of reactions that varied the aluminum content of the starting mixture.

The phases formed in select Ti−Al reactions are summarized in Table 1. By utilizing 0−23 mol of $AlCl_3$ in the reactant mixture, portions of the Ti−Al phase diagram containing Ti_3Al, TiAl, $TiAl_2$, and $TiAl_3$[39] were accessed. Variation of the aluminum content should

Table 2. Maximum Temperatures Achieved by Ti−Al Forming Single-Displacement Reactions

reactant metal molar ratios, Ti/Al	maximum reaction temperature (°C)
3:0	1086 ± 44
3:1	1062 ± 20
3:1.4	1006 ± 17
3:2	1002 ± 28
3:3	1005 ± 17
3:4	1012 ± 29
3:5	984 ± 35
3:6	962 ± 33
3:7	950 ± 28
3:8	953 ± 38
3:9	932 ± 34
3:10	905 ± 29

indicate which reactant ratios produce phase pure intermetallic compounds and what processes affect the formation of such a product. Instead, a wide range of compositions is observed in a single reaction. The phases represented in the phase diagram are merely a guideline, it is not expected that a given reactant composition will necessarily produce a single phase product. This implies that solid-state single-displacement reactions are kinetically controlled.

Control reactions were also performed separately with $TiCl_3$ and $AlCl_3$. The reaction containing $TiCl_3$ was self-propagating. The reaction containing only $AlCl_3$ did not propagate in the reaction cell. With a maximum adiabatic temperature of 1100 °C, the reaction $AlCl_3 + 1.5Mg \rightarrow Al + 1.5MgCl_2$ was expected to propagate. However, while the reduction of $AlCl_3$ to aluminum by magnesium is thermodynamically favorable, the thermal transfer characteristic of the reaction vessel likely dissipates the heat generated by the aluminum forming reaction fast enough to prevent propagation. In some cases, thermal dissipation is desirable, such as to prevent decomposition.[31] However, in this reaction, a dissipation of thermal energy results in reduced preheating. This ultimately stops the reaction from fully propagating.

In all reactions studied, five major phases: Ti, Ti_3Al, TiAl, $TiAl_3$, and Al were identified by powder X-ray diffraction. As the $AlCl_3$ content in the reactant mixture was increased, the measured maximum reaction temperature (T_{max}) decreased (Table 2) and the resulting products contained more aluminum-rich phases. The most aluminum-rich products were found to contain only $TiAl_3$ and Al as detected by X-ray diffraction, which does not give a quantitative measure of the bulk composition of the powders produced. It can be seen from Table 1 that the measured titanium content matches the expected content in only a few reactions, but it is within 10% of theoretical for most of them. This is likely due to several factors, including nonuniform propagation, oxidation of the product, preferential loss of Ti, loss of unreacted $TiCl_3$ during workup, and adsorption of atmospheric water in the product while it was stored.

It has been shown, for solid-state high-temperature synthesis reactions, that there exist several modes of nonuniform propagation.[39] For Ti−Al reactions initiated with a Nichrome filament, the cover was removed from the reaction vessel and the progress of the reaction was observed visually. For some reactions, typically those with a higher $AlCl_3$ content, a nonuniform reaction propagation was observed. This phenomena may result in partially unreacted portions of the reaction mixture. Any unreacted $TiCl_3$ (or $AlCl_3$) would be removed in the subsequent ethanol washes. This would make the amount of titanium detected in the sample lower than expected.

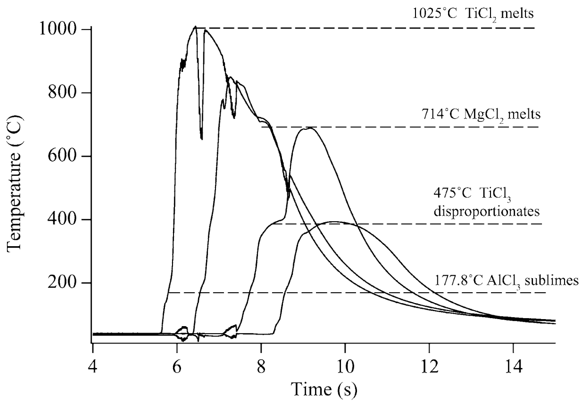

Figure 6. Thermal profiles elucidating the reaction mechanism for Ti/Al single-displacement reactions. The reaction shown contains a molar ratio of 3:23:39 $TiCl_3/AlCl_3/Mg$ and does not go to completion. The phase changes indicate the progress of the reaction. Thermocouple one reaches a maximum temperature of 1025 °C, the melting point of $TiCl_2$. Thermocouple three reaches a maximum temperature of 714 °C, the melting point of $MgCl_2$. Thermocouple four reaches a maximum temperature near 475 °C, the disproportionation temperature of $TiCl_3$. This event is also evident in the profile for thermocouple three.

Reaction Propagation Analysis. To discuss the mechanism of reaction propagation, it is useful to examine the upswing of typical reaction temperature profiles. For reactions containing a low aluminum content, the temperature rise is so fast that many features are lost even at a sampling resolution of 1 ms. The reaction can be slowed by the addition of an inert diluent (such as $MgCl_2$) or by addition of more $AlCl_3$. For example, a reaction with 23 mol of $AlCl_3$ could be initiated, but only propagated partially through the reaction vessel. The temperature of the reaction front decreased steadily as the reaction progressed through the mixture (Figure 6). This indicates that the thermal input from the reaction was overcome by the thermal dissipation of the reaction cell. In fact, the various steps in the mechanism of the co-reduction process can be determined from these reaction data. The initial part of the curve shows changes in the heating rate at about 178 and 475 °C. These values correspond to the sublimation of $AlCl_3$ and disproportionation of $TiCl_3$, respectively. Additionally, the data from the stalled reaction can be used to further ascertain that 714 and 1025 °C (the melting points of $MgCl_2$ and $TiCl_2$, respectively) are also important in the mechanism of the reaction. Also observed in Figure 3 is the change in cooling rate at about 700 °C. This is likely due to the solidification of $MgCl_2$ and the subsequent change in heat transfer characteristics of the material. From this information the mechanism can be described as follows. Preheating

---

(39) Mukasyan, A. S.; Rogachev, A. S.; Varma, A. *Chem. Eng. Sci.* **1999**, *54*, 3357−3367.

from the reaction front causes $AlCl_3$ to sublime, initiating the reaction. The $AlCl_3$ vapor reacts with Mg releasing heat to further the completion of the reaction. However, this step is not the main driving force for propagation. This can be surmised from the fact that a reaction containing $AlCl_3$ alone does not propagate. The heat released from this reaction causes the temperature to rise to the disproportionation temperature of $TiCl_3$. At this point, $TiCl_3$ decomposes to $TiCl_4$ gas and $TiCl_2$ solid. The $TiCl_4$ gas is then free to diffuse through the reaction mixture. It has been found that a tightly packed reaction mixture will not propagate. Because $TiCl_4$ will not be able to diffuse into unreacted portions of a tightly packed mixture, this gas is likely the main mode by which the reaction propagates. The reactivity of $TiCl_4$ toward Mg was determined by mixing liquid $TiCl_4$ with Mg powder and initiating a reaction with a heated Nichrome wire. The resulting reaction not only produced Ti metal and $MgCl_2$ as expected, but also $TiCl_3$ as given in eq 3.

$$3TiCl_4 + 3Mg \rightarrow Ti + 2TiCl_3 + 3MgCl_2 \qquad (3)$$

It can be surmised that a similar reaction is occurring in the reaction mixture. As the $TiCl_4$ diffuses into unreacted portions of the mix it reacts with Mg, forming $TiCl_3$ and Ti metal. This generates sufficient heat to continue reaction propagation. The heat generated by the reduction of $AlCl_3$ and $TiCl_4$ is enough to melt the $MgCl_2$ product. When enough heat is generated to melt $TiCl_2$, reduction can occur, and the remainder of the Ti is produced. The final amount of heat is liberated with the formation of a Ti–Al intermetallic phase.

The mode of propagation indicates a probable reason for the low Ti content in the mixtures produced. The reaction vessel is not sealed. This design allows gaseous $TiCl_4$ not only to flow into the unreacted reaction mix, but also to flow out the sides of the vessel and out of the reaction area.

Along with thermocouples, platinum electrodes were embedded in the reaction mixture. It was found that solid-state single-displacement reactions can produce an electric pulse as the reaction front intercepts an individual set of electrodes. This phenomena has been observed in solid-state high-temperature synthesis reactions[40] and dubbed a chemoelectric field. It has been attributed to the reduction of metal ions to produce neutral metal atoms. These electrodes were also used as a further gauge of propagation rate. Although the electrical signal in itself is useful, the magnitude of the electrode signal does not appear to yield useful information. The spike comes from the signal produced by the reaction volume between the two electrodes. However, on a small scale the reaction is not a completely uniform process and the signal can vary significantly in magnitude from one experiment to another.

Because the product of the reaction is conductive, an intersection of the reaction front with either a thermocouple or an electrode supplies a path to ground for the electrons produced. This means that the electrodes and thermocouples that are embedded in reacted portions of the mixture will respond to fields produced by the reaction front intersecting either the thermocouples or electrodes. By examining the onset of the electrical signal in relation to the temperature profile (cf., Figure 4), it can be seen that a chemical reaction occurs after $AlCl_3$, in the reaction zone, melts. By comparing the width of electrical pulses (cf., Figure 5), the length of the reaction front can be estimated. If we assume that the reaction is proceeding only when there is an electric field being generated, then the reaction duration can also be estimated. Typically, a 400-ms reaction duration is observed. By measuring the peak distances of the temperature profiles, a reaction propagation rate and propagation zone width can be determined. This zone is termed the combustion front. Measurements of this zone in solid-state high-temperature synthesis reactions[41] have given a range of 0.05 to 0.50 mm for its width. The derived width of the single-displacement reaction zone (~0.5 mm, see results) is comparable to the upper part of the SHS range.

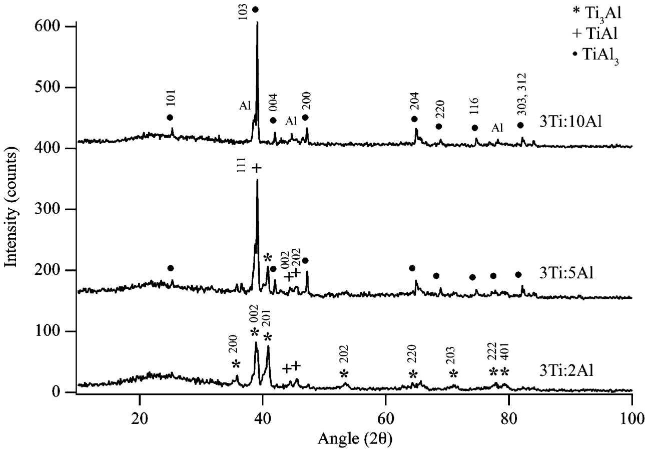

Figure 7. Powder X-ray diffraction patterns demonstrating phase control in the Ti–Al system. Single-displacement reactions with different molar ratios of Ti/Al/Mg are shown: (A) 3:2:7.5, (B) 3:512, and (C) 3:10:19.5. The Miller indices for $TiAl_3$, TiAl, and Ti_3Al are given on the top, middle, and bottom graphs, respectively.

It was noted that reactions involving $TiCl_3$ produce macroscopic- and microscopic-scale filaments (Figure 2). These filaments show dendritic growth. In view of the mechanism involved in the propagation of $TiCl_3$-containing reactions it is reasonable to infer that microfilament formation is a result of the reduction of gaseous $TiCl_4$.

Traditionally, SSM reactions have been initiated by applying current to a Nichrome fuse embedded in the reaction mixture.[42] This creates a reaction zone that propagates through the unreacted mixture. The result is a product that is controlled by the dynamics of the reaction propagation. These dynamics are controlled by such parameters as the thermal conductivity of the reaction vessel and the mobility of reaction intermediates. Utilizing such an initiation technique, the Ti–Al phases of Ti_3Al, TiAl, and $TiAl_3$ have been accessed (see Figure 7). It is easiest to produce a pure phase of $TiAl_3$ by Nichrome wire ignition.

It has been shown that intermetallic phases can be produced by SHS reactions initiated with microwave

---

[40] Morozov, Y. G.; Kuznetsov, M. V.; Merzhanov, A. G. *Int. J. Self-Propag. High-Temp. Synth.* **1997**, *6*, 1–13.

[41] Varma, A. *Sci. Am.* **2000**, *283*, 58–61.

[42] Kaner, R. B.; Bonneau, P. R.; Gillan, E. G.; Wiley, J. B.; Jarvis, R. F., Jr.; Treece, R. U.S. Patent 5110768, 1992; p 7.

energy.[43] In the current reactions, the microwave-initiated products were compared to the same reaction mixtures initiated with a Nichrome wire (Table 1). The differences in products can be explained by examining the propagation mechanisms and initiation profiles of the reactions. In a Nichrome wire initiated reaction, a single combustion front proceeds through the reactant mixture. This can be slow (seconds) or fast (milliseconds). During this propagation, reactant material ahead of the propagation front is subject to preheating. This can lead to premature decomposition of reactant or migration of reactant from the reaction zone. The resulting product would be deficient in said reactant. This can be seen in the $3Ti{\cdot}nAl$ reactions which produce products with Ti phases that are aluminum rich. In a microwave reaction, the microwave energy produces hot spots throughout the reaction mixture. These hot spots can lead to multiple initiation events. The result is a reaction that propagates from multiple origins.[44] This gives a more rapid completion time. A second consequence of this is that there is less time for crystallite growth through Ostwald ripening; thus smaller crystallites are observed. In addition, multiple propagation fronts limit the amount of material subject to preheating.

LiAl can also be utilized as a precursor species in the production of intermetallics in the Ti−Al system by solid-state metathesis (SSM) reactions. Analysis of the products of the reaction between LiAl and $TiCl_3$ by XRD indicates that the only crystalline phase generated is $TiAl_3$. This is in agreement with the results from the single-displacement reaction using $TiCl_3$ and $AlCl_3$. Direct measurements of the reaction temperature profile in the $TiCl_3$/LiAl system were recorded with an in situ thermocouple. The initial temperature rise after precursor ignition is extremely fast. This is characteristic of many rapid SSM and other combustion-like reaction systems. The peak temperature is 1300 °C and occurs within 260 ms after ignition. This is faster than the temperature rise observed in Ti−Al producing single-displacement reactions, which is on the order of 700 ms. The cooling curve is also quite fast, with temperatures dropping below the melting point of the LiCl byproduct (mp = 610 °C) within 8 s. There are two isothermal regions on the cooling curve, one at approximately 1200 °C and the other near 600 °C. The high-temperature region approaches the solidification point of molten $TiAl_3$ (mp = 1350 °C), whereas the lower-temperature region likely corresponds to the solidification of the LiCl (mp = 610 °C) melt.

Conclusions

Ti−Al intermetallics including Ti_3Al, TiAl, and $TiAl_3$ have been successfully synthesized by single- and double-displacement solid-state reactions. Through the use of in situ measurements the reactions were studied in some detail. These measurements allowed the elucidation of the propagation mechanism for Ti−Al producing single-displacement reactions. Because these are redox reactions, they can be monitored (by observing potentials produced during the reaction) with platinum electrodes embedded in the reaction mixture. This has allowed thermal events in the reaction propagation to be correlated with chemical events in the reaction itself. It was found that chemical processes commence upon the sublimation of $AlCl_3$. Propagation of the reaction is dependent upon the disproportionation of $TiCl_3$ to $TiCl_4$ and $TiCl_2$. The production of $TiCl_4$ results in a gaseous intermediate that is free to diffuse into unreacted portions of the mixture. The production of $TiCl_2$ limits the maximum temperature of single-displacement reactions to 1025 °C. In contrast, double-displacement reactions involving LiAl are energetic enough to reach 1300 °C, the boiling point of LiCl. The formation of a single-phase product is governed by factors such as reactant mobility, reaction inhomogeneity, and reaction speed. The use of microwave energy initiates simultaneous reaction fronts and results in products that are closer to the expected titanium content and phase composition.

The simplicity of the Ti−Al forming reactions studied shows promise for the development of solid-state routes to other intermetallic compounds. Ab initio calculations have been performed to identify the most stable binary intermetallic compounds.[45] Of the compounds identified, TiAl, and $TiAl_3$ were produced by single-displacement reactions. The stability of these intermetallic compounds, as expressed by their high heats of formation, may help to explain the success in forming these compounds by displacement reactions. This may also explain the dominance of these products in reactions that were not expected to generate them.

Acknowledgment. We thank Jiaxing Huang for assistance with transmission electron microscope images, and Eric Hemminger for assistance in developing in situ reaction temperature measurements. This work is supported by the National Science Foundation grant DMR-0073581 and its Research Experience for Undergraduates program grant DMR-0132226.

CM021829A

---

(43) Gedevanishvili, S.; Agrawal, D.; Roy, R. *J. Mater. Sci. Lett.* **1999**, *18*, 665−668.

(44) Clark, D. E.; Iftikhar, A.; Dalton, R. C. PCT Int. Appl. 9013513; 1990; p 43.

(45) Johannesson, G. H.; Bligaard, T.; Ruban, A. V.; Skriver, H. L.; Jacobsen, K. W.; Norskov, J. K. *Phys. Rev. Lett.* **2002**, *88*, 255506/255501−255506/255505.